Texture Image Segmentation using a New Descriptor and Mathematical Morphology

Idrissi Sidi Yassine and Samir Belfkih
Faculty of Science and Technology, Sidi Mohamed Ben Abdellah University, Morocco

Abstract: *In this paper we present a new texture descriptor based on the shape operator defined in differential geometry. Then we describe the texture feature analysis process based on the spectral histogram. After that we describe a new algorithm for texture segmentation using this descriptor, statistics based on the spectral histogram, and mathematical morphology. Many results are presented to illustrate the effectiveness of our approach.*

Keywords: *Textures segmentation, spectral histogram, differential geometry, mathematical morphology.*

Received December 19, 2010; accepted May 24, 2011

1. Introduction

Texture image segmentation is a fundamental problem in computer vision with a wide variety of applications. The texture can be regarded as a similarity grouping in an image. The local sub-pattern properties give rise to the perceived lightness, uniformity, density, roughness, regularity, linearity, frequency, phase, directionality, coarseness, randomness, fineness, smoothness, granulation, etc. Because texture is regarded as a rich of source of visual information, it is difficult to define the properties that can be used effectively to characterize all textures and to find a set of properties that can be used to distinguish textures found in a given image. And it is also difficult to determine the texture region boundary accurately because the texture is a region property rather than a point property.

The common approaches to solve the textured image segmentation problem can be classified to be either supervised or unsupervised algorithm based on whether the number of textures contained in the image is known in advance or not. The typical methods are region growing, estimation theory based on maximum likelihood, split-and-merge, bayesian classification, probabilistic relaxation, clustering, the mumford-shah model, etc.

In this paper, we choose the spectral histograms as the texture feature and adopt an effective computing method to evaluate the similarity between histograms. Spectral histogram consists of histograms of response images of chosen filters. It can capture local spatial patterns through filtering and global patterns through histograms and constraints among different filters compared with the above texture analysis methods. Based on the determined texture features, we can obtain the initial segmentation result. Skeleton extracting algorithm based on mathematical morphology is applied to determine the texture region boundary accurately. The outline of our paper is as follows: In section 2, we introduce the intrinsic texture descriptor. Then in section 3, we describe the texture feature analysis process based on the spectral histogram. In section 4, skeleton extracting algorithm applied to obtain the accurate texture region boundary. Experimental results are shown and discussed in section 5. Finally, section 6 gives the conclusion.

2. New Texture Descriptor

2.1. Previous Work

In this work, we are particularly interested in the Beltrami representation introduced by [11]. Sochen *et al.* [11], proposed a new efficient representation of images by considering images as a riemannian manifold embedded in a higher dimensional space. For instance, a standard 2 dimensional gray value image $I:IR^2 \rightarrow IR^+$ can be viewed as a surface $\sum$ with local coordinates (x,y) embedded in IR^3 by a smooth mapping:

$$X:(x,y) \rightarrow (X_1 = x, X_2 = y, X_3 = I(x,y)) \quad (1)$$

This manifold-based representation of images offers two main advantages. Firstly, it allows to use efficient tools borrowed from differential geometry to perform different image processing tasks such as denoising or segmentation as we will do in this paper. The second main advantage is the ability to work with arbitrary N dimensional images.

Sagiv *et al.* [9] used the Beltrami framework to represent the texture image as a *2-D* dimensional manifold embedded in a space of $N+2$ dimensions, where N is the number of Gabor responses. They used the first fundamental form [7], also called metric tensor, of the texture manifold to define an intrinsic edge detector like in [10]. The idea of using the metric

tensor to intrinsically define the edges between different homogeneous texture regions is efficient in the context of differential geometry. Indeed, the first fundamental form describes the distortion or rate of change of the manifold and so can detect boundary between different parts of the manifold corresponding to different homogeneous textures. More precisely Caselles *et al.* [3], used the geodesic active contour model to drive the evolving contour toward the boundaries between two different texture regions by considering the edge detector function or stopping function as the inverse of the determinant of the metric tensor. This can be explained in the following way. If we consider the definition of the first fundamental form:

$$g_{\mu\nu} = \left(< \frac{\partial X}{\partial \mu}, \frac{\partial X}{\partial \nu} > \right) \tag{2}$$

where $\mu,\nu=x,y$ in the (x, y)-basis, we have in the case of gray scale images, $X=(x,y,I)$ and $g_{xx}=1+I_x^2$, $g_{xy}=I_xI_y$ and $g_{yy}=1+I_y^2$ which $det(g_{\mu\nu})=(1+|\nabla I|^2)$. The previous function exactly corresponds to the edge detector function used in the standard model [3]. Thus, Caselles *et al.* used the metric tensor of texture images to define an efficient edge detector for textural images. Nevertheless, as we said earlier, the edge detector function is not robust enough to segment a wide range of images and a region-based term, coming from the vectorial Chan-Vese model [4], was coupled with their intrinsic edge detector function to perform the segmentation of complex textures. This coupling is necessary because edge-based active contours are too sensitive to noise, bad contrast and initial position. Hence, one of the goals of this paper is to define a region descriptor/feature, instead of a boundary descriptor, for textural regions. Like [9], we also wish to develop an intrinsic descriptor based on the geometrical shape of the manifold representing the texture region. We thus propose to use the shape operator and more specifically the eigenvalues of the shape operator to describe the geometry of the textures of interest. The shape operator is a linear operator which calculates the bending of a surface in different directions [5].

The eigenvalues of the shape operator correspond to the extremal of bending of the surface, they are called principal curvatures and they are known to represent the geometry of the considered smooth manifold. Indeed, in the simple case of a curve in the space, the curvature κ of this curve is the inverse of the radius ρ of the best fitting circle to the curve, i.e., $\kappa=1/\rho$. It is then intuitive to say that the curvature describes the local shape of the curve and by extension the principal curvatures describe the manifold.

2.2. Our Proposed Descriptor

In this work, we choose to represent the texture manifold by the simplest Beltrami representation, i.e., $X=(x,y,I)$. Since texture images are seen as a *2-D* manifold, two principal curvatures can be computed in this representation, namely (κ_1,κ_2).

Let us introduce the mathematical definition of the shape operator that we call *S*. The shape operator measures the shape of the manifold in a given region by estimating how the normal N_Σ to the surface $\sum$ changes from point to point.

We refer to [5, 7] for definitions and the following property:

Let $\sum$ be a regular surface, and let N_Σ be a surface normal to $\sum$ defined in a neighborhood of a point $p \in \sum$. For a tangent vector V_p to $\sum$ at p the shape operator is defined as:

$$S(V_p) = -D_{V_p} \mathrm{N}_\Sigma \tag{3}$$

where $D_{V_p} N_\Sigma$ is the derivative of the surface normal N_Σ in direction V_p. The eigenvalues of the shape *S* of a regular surface $\sum$ at $p \in \sum$ are precisely the principal curvatures of $\sum$ at *p*.

The corresponding unit eigenvectors are unit principal vectors, and vice versa. In our situation [7], the principal curvatures κ_1, κ_2 of the *2-D* manifold are the roots of the following equation:

$$\kappa^2 - b_{\mu\nu} g^{\mu\nu} \kappa + \frac{b}{g} = 0 \tag{4}$$

where $g^{\mu\nu}$ is the inverse metric (the inverse of the matrix of metric tensor) of $g_{\mu\nu}$, g, b are the determinant of $g_{\mu\nu}$, and $b_{\mu\nu}$ is the second fundamental form defined by:

$$b_{\mu\nu} = \left(< \frac{\partial^2 X}{\partial \mu \partial \nu}, \mathrm{N}_\Sigma > \right) \tag{5}$$

where $\mu,\nu=x,y$ in the (x, y)-basis, and the Einstein summation convention is used, which means that elements with identical subscripts and superscripts are summed over.

Let I be the original gray level image, I_x and I_y the partial derivatives. The mapping X is equal to$(x,y)\rightarrow(x,y,I(x,y))$ and the first fundamental form is thus given by:

$$g_{\mu\nu} = \begin{pmatrix} 1+I_x^2 & I_xI_y \\ I_xI_y & 1+I_y^2 \end{pmatrix} \tag{6}$$

The normal to the manifold is given by $\mathrm{N}_\Sigma = \frac{1}{Z}(-I_x,-I_y,1)$, $Z=\sqrt{1+I_x^2+I_y^2}$ which yields us to the calculus of the second fundamental form

$b_{\mu\nu} = \frac{1}{Z}\begin{pmatrix} I_{xx} & I_{xy} \\ I_{xy} & I_{yy} \end{pmatrix}$ using previous property, the values of the principal curvatures are given by:

$$\kappa_{1,2} = \left(-\beta \pm \sqrt{\beta^2 - 4\alpha\gamma}\right)/2\alpha \quad (7)$$

where $\alpha = \left(1 + I_x^2\right)^2 - I_x I_y$, $\gamma = \frac{1}{Z^2}\left(I_{xx} I_{yy} - I_{xy}^2\right)$

and $-\beta = \frac{1}{Z}\left(I_{xx}(1+I_y^2) + I_{yy}(1+I_x^2) - I_{xy} I_x I_y\right)$.

The first principal curvature $\kappa_1(\kappa_1 \geq \kappa_2)$ corresponds to the maximal change of the normal to the surface and κ_2 corresponds to the minimum change. In order to use the information provided by the two principal curvatures, we consider to work with the norm:

$$\kappa_t = \sqrt{\kappa_1^2 + \kappa_2^2} \quad (8)$$

where $\kappa_t : \Omega_0 \to \mathbb{R}^+$ defines the texture descriptor that we will use to segment regions with different texture patterns and Ω_0 corresponds to the image domain.

Figure 1. Real image and its texture described by our descriptor.

Figure 1 shows the result of our texture feature descriptor, where the tiger is more discernable from the background. In fact, almost all the background has been set to a constant value.

3. Texture Analysis

3.1. Spectral Histogram Representation

In an image I, given a window W and a chosen bank of filter $\{F^n, n=1, 2, \ldots, N\}$, we compute a sub band image W^n through a linear convolution for each filter F^n, that is: $W^n(\vec{P}) = F^n * W(\vec{P}) = \sum_{\vec{u}} F^n(\vec{u}) W(\vec{P} - \vec{u})$, where by a circular boundary condition is used for convenience, and where $\vec{P}$, and $\vec{u}$ specify pixel locations.

For W^n, we define its histogram, a bin of which is given by:

$$H_w^n(z_1, z_2) = \frac{1}{|w|} \sum_{\vec{v} \in w} \int_{z_2}^{z_1} \delta(z - W^n(\vec{P}))\, dz \quad (9)$$

where z_1, and z_2 specify the range of the bin, $\delta()$ is the Dirac delta function, $|w|$ is the size of the given image window (also called the integration scale). With respect to the chosen filters, we define the spectral histogram as:

$$H_W = (H_W^1, H_W^2, \ldots, H_W^N) \quad (10)$$

The spectral histogram of an image window or an image is essentially a vector consisting of marginal distributions of filter responses.

3.2. Similarity between Spectral Histograms

Because the spectral histogram is a probability distribution, a similarity measure between two histograms H_{W^1} and H_{W^2} can be defined as:

$$\begin{aligned} \chi^2(H_{W^1}, H_{W^2}) &= \frac{1}{|N|} \sum_{n=1}^{N} \sum_{z} \frac{\left(H_{W_1}^n(z) - H_{W_2}^n(z)\right)^2}{H_{W_1}^n(z) + H_{W_2}^n(z)} \\ &= \frac{1}{|N|} \sum_{n=1}^{N} \chi^2\left(H_{W_1}^n, H_{W_2}^n\right) \end{aligned} \quad (11)$$

where $\chi 2$-statistic is a first-order approximation of the Kullback-Leibler divergence and used widely to compare histograms. The spectral histogram integrates responses from different filters and provides a naturally normalized feature statistic to compare image windows or images of different sizes. That is, they do not need to be aligned. By implicitly integrating geometrical and photometric structures of textures, the spectral histogram provides a sufficient model for characterizing perceptual appearance of textures.

In [12] Xiamen compute the spectral histogram centered at a pixel location. We adopt a method different from [12] when computing the similarity between histograms for each pixel in an image.

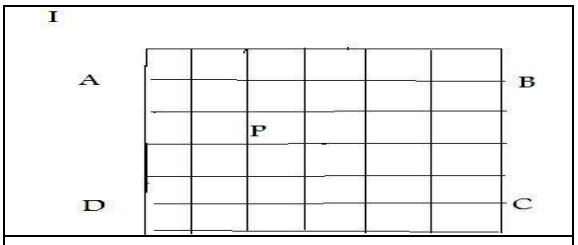

Here P is a pixel in an image. The solid is an image I. The dotted are four corner windows with the size 3×3 corresponding to P, where A represents top-left one, B represents top-right one, C represents bottom-right ones and D represents bottom-left one.

Figure 2. Windows for similarity computation.

As shown in Figure 2, $\vec{P}$ is a pixel in an image, there are four windows corresponding to $\vec{P}$ Top-left window is represented by A, B represents top right window, C represents bottom-right window, and D represents bottom-left window.

Let:

$$b_{\vec{P}_x} = \chi_{\vec{P}}^2\left(H_{W_A}, H_{W_C}\right) \quad (12)$$

$$b_{\vec{P}_y} = \chi_{\vec{P}}^2\left(H_{W_B}, H_{W_D}\right) \quad (13)$$

The similarity between spectral histograms for the pixel $\vec{P}$ is determined by the formula:

$$b_{\vec{P}}^2 = b_{\vec{P}_x}^2 + b_{\vec{P}_y}^2 \tag{14}$$

3.3. Implementation Issues

Because a spectral histogram is defined with respect to a bank of filters, the first implementation issue is what filters should be selected so that various textures can be considered effectively.

In addition to our descriptor we adopt four types of filters suggested from the studies of visual perception and the empirical studies of independent components of natural images [1, 8]:

1. The intensity filter, which is the $\delta()$ function and captures the intensity value at a given pixel.
2. Difference filters. We use four of them:

$$D_x=[0\text{-}11],\ D_y=[0\text{-}11],\ D_{xx}=[\text{-}12\text{-}1],\ D_{yy}=[\text{-}12\text{-}1] \tag{15}$$

3. Laplacian of Gaussian filters:

$$LoG(x,y\,|\,T)=(x^2+y^2-T^2)\exp(-\frac{x^2+y^2}{T^2}) \tag{16}$$

where $T=\sqrt{2}\delta$ determines the scale of the filter and δ is the variance of the Gaussian function.

4. Gabor filters:

$$\begin{aligned} Gabor(x,\,y\,|\,T,\,\theta) &= \exp(-\frac{1}{2T^2}(4(x\sin\theta+y\cos\theta)^2+(x\cos\theta+y\sin\theta)^2)) \\ &\exp(-i\frac{2\pi}{T}(x\cos\theta+y\sin\theta)) \end{aligned} \tag{17}$$

where T is a scale.

These filters provide efficient ways of extracting spatial structures at different orientations and frequencies and empirically have shown to be effective for different kinds of textures. In our implementation, the range of image data firstly is unified to the range [0, 1], and the number of bins is specified as a parameter for each filter, thus the filter responses range is also divided into the given number of bins evenly. So the measurement between marginal distributions can be done on the same basis.

4. Boundary Localization

The initial segmentation can be done by binary operation for the feature image. Then we employ the skeleton extraction based on medial axis transform to locate the boundary of texture region accurately. For medial axis transform, we apply morphologic operations. Distance transform can then be defined in terms of erosions and openings. The morphological skeleton S of an image I can be calculated using the following:

$$S(I)=\bigcup_{k=0}^{K} S_k(I) \tag{18}$$

with:

$$s_k(I)=(I\odot kB)-((I\odot kB)\circ B) \tag{19}$$

where B is a structuring element, $(I\odot kB)$ means $k\geq 0$ successive erosions of I by B, $I\circ B$ means the opening of I by B, K is the number of the last iterative step before I erodes to an empty set.

5. Results

In the above experiment, for LoG filter, $\delta=\frac{2}{\sqrt{2}},\frac{5}{\sqrt{2}}$, for Gabor filter, $T=6$, $\theta=30^\circ,90^\circ,150^\circ$; the bins of the histogram is set 11. We present some results on real and synthetic images (Brodatz textures):

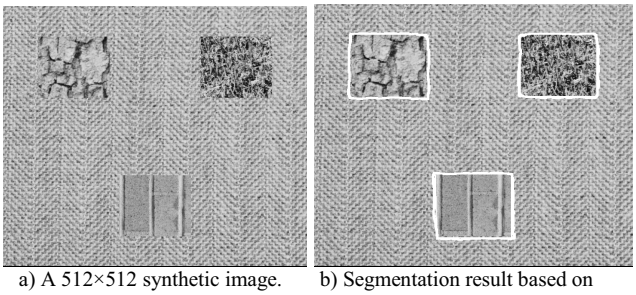

a) A 512×512 synthetic image. b) Segmentation result based on the skelecton extraction.

Figure 3. Distinguish the three regions from the background.

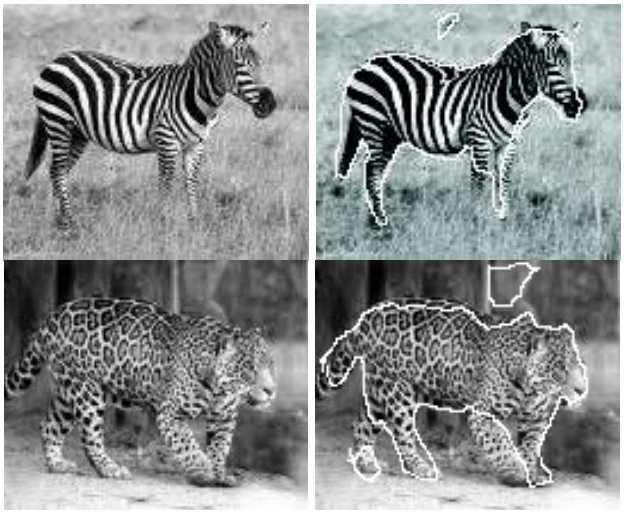

a) A 122×109 original image. b) Segmentation result based on the skelecton extraction.

Figure 4. Natural images.

In Figure 3, our algorithm has managed to distinguish the three regions from the background, because it is based on probability density which is different for the three regions. In Figure 4, as natural images, we have chosen the segmentation of a zebra and a leopard picture which presents textured features, the segmentation results are satisfactory.

6. Conclusions

We have presented a texture segmentation algorithm which uses a new descriptor, spectral histogram and

skeleton extracting. The segmentation results are visually satisfactory. The advantage of using the skeleton extracting to solve the textured image segmentation is no need of given seed pixels or knowing the number of regions.

References

[1] Bell A. and Sejnowski T., "The Independent Components of Natural Scenes are Edge Filters," *Vision Research*, vol. 37, no. 23, pp. 3327-3338, 1997.

[2] Bresson X., Esedoglu S., Vandergheynst P., Thiran J., and Osher S., "Fast Global Minimization of the Active Contour/Snake Model," *Journal of Mathematical Imaging and Vision*, vol. 28, no. 2, pp. 151-167, 2007.

[3] Caselles V., Kimmel R., and Sapiro G., "Geodesic Active Contours," *International Journal of Computer Vision*, vol. 22, no. 1, pp. 61-79, 1997.

[4] Chan T., Sandberg B., and Vese L., "Active Contours without Edges for Vector-Valued Images," *Journal of Visual Communication and Image Representation*, vol. 11, no. 2, pp. 130-141, 2000.

[5] Gray A., *Modern Differential Geometry of Curves and Surfaces with Mathematica*, CRC Press, USA, 1996.

[6] Hasanul K., Abdullah A., and Oksam C., "Brightness Preserving Image Contrast Enhancement using Weighted Mixture of Global and Local Transformation Functions," *The International Arab Journal of Information Technology,* vol. 7, no. 4, pp. 403-410, 2010.

[7] Kreyszig E., *Differential Geometry*, Dover Publications, New York, 1991.

[8] Olshausen B. and Field D., "Emergence of Simple-Cell Receptive Field Properties by Learning a Sparse code for Natural Images," *Nature*, vol. 381, no. 6583, pp. 607-609, 1996.

[9] Sagiv C., Sochen N., and Zeevi Y., "Integrated Active Contours for Texture Segmentation," *IEEE Transactions on Image Processing*, vol. 15 no. 6 pp. 1633-1646, 2006.

[10] Sapiro G., "Color Snakes," *Computer Vision Image Understanding*, vol. 68, no. 2, pp. 247-253, 1997.

[11] Sochen N., Kimmel R., and Malladi R., "A General Framework for Low Level Vision," *IEEE Transactions on Image Processing*, vol. 7, no. 3, pp. 310-318, 1998.

[12] Xiamen L. and DeLiang W., "Image and Texture Segmentation Using Local Spectral Histograms," *IEEE Transactions on Image Processing*, vol. 15, no. 10, pp. 3066-3077, 2006.

[13] Xiuwen L. and DeLiang W., "Texture Classification Using Spectral Histograms," *IEEE Transactions on Image Processing*, vol. 12, no. 6, pp. 661-670, 2003.

Idrissi Sidi Yassine after spending my license study on applied mathematics, statistics options, I continued my depth studies on applied mathematics, scientific computing option. In this previous education, I've learned about the most important knowledge on applied mathematics, and I acquired a lot of skills in programming language, image processing, operating systems, and software. I also realize some important projects concerning conducting a library for image processing (in C + +), and description some algorithms for solving PDEs by the finite element method and optimization. This various academic career allows me to continue and success my doctoral studies.

Samir Belfkih research director in image processing and computer sciences. Professor in Department of Computer Science. Faculty of Science and Technology, University Sidi Mohammed Ben Abdellah Fez, Morocco My general interests are in the areas of communications, application the partial differential equation in image processing, detection and restoration, teleradiology. Current research topics focus on cyber security, wireless communications, image processing applied on medical images, and intelligence of information systems.